Article:
Malpetti, M., Roemer, S.N., Harris, S. et al. (2024) Neuroinflammation parallels 18F-PI-2620 positron emission tomography patterns in primary 4-repeat tauopathies. Movement Disorders, 39 (9). pp. 1480-1492. ISSN: 0885-3185

https://doi.org/10.1002/mds.29924

RESEARCH ARTICLE

Neuroinflammation Parallels 18F-PI-2620 Positron Emission Tomography Patterns in Primary 4-Repeat Tauopathies

Maura Malpetti, PhD,[1*] Sebastian N. Roemer, MD,[2,3] Stefanie Harris, MD,[4] Mattes Gross,[3,4] Johannes Gnörich, MD,[4] Andrew Stephens, MD, PhD,[5] Anna Dewenter, PhD,[3] Anna Steward, MSc,[3] Davina Biel, PhD,[3] Amir Dehsarvi, PhD,[3] Fabian Wagner,[3] Andre Müller, MD,[5] Norman Koglin, MD,[5] Endy Weidinger, MD,[2] Carla Palleis, MD,[2,6,7] Sabrina Katzdobler, MD,[2] Rainer Rupprecht, MD,[8] Robert Perneczky, MD,[6,7,9,10,11] Boris-Stephan Rauchmann, MD,[9,12] Johannes Levin, MD,[2,6,7] Günter U. Höglinger, MD,[2,6,7] Matthias Brendel, MD,[4,6,7] and Nicolai Franzmeier, PhD[3,6,13]

[1]*Department of Clinical Neurosciences and Cambridge University Hospitals NHS Trust, University of Cambridge, Cambridge, UK*
[2]*Department of Neurology, LMU Hospital, LMU Hospital, LMU Munich, Munich, Germany*
[3]*Institute for Stroke and Dementia Research, LMU Munich, Munich, Germany*
[4]*Department of Nuclear Medicine, LMU Hospital, LMU Munich, Munich, Germany*
[5]*Life Molecular Imaging, Berlin, Germany*
[6]*Munich Cluster for Systems Neurology (SyNergy), Munich, Germany*
[7]*German Center for Neurodegenerative Diseases (DZNE) Munich, Munich, Germany*
[8]*Department of Psychiatry and Psychotherapy, University Regensburg, Regensburg, Germany*
[9]*Department of Psychiatry and Psychotherapy, LMU Hospital, LMU Munich, Munich, Germany*
[10]*Aging Epidemiology Research Unit, School of Public Health, Imperial College London, London, UK*
[11]*Sheffield Institute for Translational Neuroscience, University of Sheffield, Sheffield, UK*
[12]*Department of Neuroradiology, LMU Hospital, LMU Munich, Munich, Germany*
[13]*Department of Psychiatry and Neurochemistry, Institute of Neuroscience and Physiology, University of Gothenburg, The Sahlgrenska Academy, Gothenburg, Sweden*

ABSTRACT: Background: Preclinical, postmortem, and positron emission tomography (PET) imaging studies have pointed to neuroinflammation as a key pathophysiological hallmark in primary 4-repeat (4R) tauopathies and its role in accelerating disease progression.

Objective: We tested whether microglial activation (1) progresses in similar spatial patterns as the primary pathology tau spreads across interconnected brain regions, and (2) whether the degree of microglial activation parallels tau pathology spreading.

Methods: We examined in vivo associations between tau aggregation and microglial activation in 31 patients with clinically diagnosed 4R tauopathies, using 18F-PI-2620 PET and 18F-GE180 (translocator protein [TSPO]) PET. We determined tau epicenters, defined as

***Correspondence to:** Dr. Maura Malpetti, Department of Clinical Neurosciences, University of Cambridge, Herchel Smith Building, Forvie Site, Robinson Way, Cambridge Biomedical Campus, Cambridge CB2 0SZ, UK. E-mail: mm2243@medschl.cam.ac.uk

Maura Malpetti, Sebastian N. Roemer, and Stefanie Harris contributed equally to this work.

Johannes Levin, Günter U. Höglinger, Matthias Brendel, and Nicolai Franzmeier contributed equally to this work.

Relevant conflicts of interest/financial disclosures: Nothing to report.

Funding agencies: M.M. was supported by Race Against Dementia and Alzheimer's Research UK (ARUK-RADF2021A-010) and the National Institute for Health and Care Research (NIHR) Cambridge Biomedical Research Centre (NIHR203312, BRC-1215-20014: the views expressed are those of the authors and not necessarily those of the NIHR or the Department of Health and Social Care). R.P. was supported by the German Center for Neurodegenerative Disorders (Deutsches Zentrum für Neurodegenerative Erkrankungen), the Hirnliga e.V. (Manfred-Strohscheer Stiftung), and the Deutsche Forschungsgemeinschaft (DFG; 1007 German Research Foundation) under Germany's Excellence Strategy within the framework of 1008 the Munich Cluster for Systems Neurology (EXC 2145 SyNergy ID 390857198), the NIHR Sheffield Biomedical Research Centre (NIHR203321), the University of Cambridge–Ludwig-Maximilians-University Munich Strategic Partnership within the framework of the German Excellence Initiative and Excellence Strategy, the European Commission under the Innovative Health Initiative program (project 101132356), the Davos Alzheimer's Collaborative, the Robert-Vogel-Foundation, the VERUM Foundation, and the Pesl-Alzheimer-Foundation. C.P. was supported by the DFG under Germany's Excellence Strategy within the framework of the Munich Cluster for Systems Neurology (EXC 2145 SyNergy ID 390857198), the Lüneburg Heritage, Friedrich-Baur-Stiftung, and Thiemann Foundation. N.F. was supported by funding from the German Parkinson Society.

Received: 19 February 2024; **Revised:** 25 June 2024; **Accepted:** 26 June 2024

Published online in Wiley Online Library (wileyonlinelibrary.com). DOI: 10.1002/mds.29924

subcortical brain regions with highest tau PET signal, and assessed the connectivity of tau epicenters to cortical regions of interest using a 3-T resting-state functional magnetic resonance imaging template derived from age-matched healthy elderly controls.

Results: In 4R tauopathy patients, we found that higher regional tau PET covaries with elevated TSPO-PET across brain regions that are functionally connected to each other ($\beta = 0.414$, $P < 0.001$). Microglial activation follows similar distribution patterns as tau and distributes primarily across brain regions strongly connected to patient-specific tau epicenters ($\beta = -0.594$, $P < 0.001$). In these regions, microglial activation spatially parallels tau distribution detectable with 18F-PI-2620 PET.

Conclusions: Our findings indicate that the spatial expansion of microglial activation parallels tau distribution across brain regions that are functionally connected to each other, suggesting that tau and inflammation are closely interrelated in patients with 4R tauopathies. The combination of in vivo tau and inflammatory biomarkers could therefore support the development of immunomodulatory strategies for disease-modifying treatments in these conditions.

Key Words: inflammation; Tau; PET; fMRI; 4R tauopathies

Progressive supranuclear palsy (PSP) and corticobasal degeneration (CBD) are fatal neurodegenerative tauopathies, characterized by the progressive decline of motor and cognitive function.[1,2] The core pathognomonic hallmark across PSP and CBD is the aggregation of misfolded hyperphosphorylated 4-repeat (4R) tau deposits (ie, a protein typically involved in microtubule assembly and stability) within neurons, astrocytes, and oligodendroglia, which spread progressively across connected brain regions, with ensuing neurodegeneration and clinical worsening.[3-7] Besides the aggregation and progressive spread of 4R tau, neuroinflammation and microglial activation have been increasingly recognized as pathophysiological hallmarks in PSP and CBD that may be critical for disease progression.[8-13] Specifically, (1) microglia and proinflammatory cytokines are upregulated in 4R tau vulnerable regions in patients with PSP and CBD,[14,15] (2) genome-wide association studies have identified *LRRK2* (*leucine-rich repeat kinase 2*) genetic variants related to neuroinflammation as risk factors for disease progression in PSP,[16,17] and (3) stronger neuroinflammation has been shown to predict faster clinical deterioration in patients with PSP.[8] Evidence from postmortem and animal studies suggests further that microglial activation and the aggregation of 4R tau may be closely linked mechanistically, because neuroinflammation not only colocalizes with tau pathology[10,15] but also acts as an important accelerator of tau aggregation and the putative transneuronal spread of tau, for example, via nuclear factor-κB signaling.[18,19] Similarly, studies in Alzheimer's disease (AD), that is, a secondary amyloid-β-associated 3/4R tauopathy, have shown that microglial activation may trigger tau hyperphosphorylation, aggregation, and spread.[20,21] Thus, microglial activation may actively contribute to the aggregation and transneuronal spreading of tau in primary tauopathies and therefore represent a candidate therapeutic target for attenuating tau aggregation and spread.

Previous imaging studies have confirmed preclinical and postmortem evidence on the colocalization and associations between tau pathology and microglial activation in PSP and CBD, and their role in accelerating disease progression.[8,10,22] Yet, no previous study has tested whether microglial activation follows similar connectivity-mediated progression patterns as for tau pathology in patients with 4R tauopathies, and whether the degree of microglial activation parallels the distribution and spreading of tau pathology across connected brain regions. To this end, we combined GE180 translocator protein–positron emission tomography (TSPO-PET), PI-2620 tau-PET, and resting-state functional magnetic resonance imaging (fMRI) in a cohort of 31 patients with clinically diagnosed PSP or corticobasal syndrome (CBS; ie, amyloid-negative to exclude AD-type tau) with assumed underlying 4R tau pathology as a cause of their clinical syndromes. We specifically used the second-generation PET ligand PI-2620, which has been shown to bind to 4R tau deposits in PSP/CBS patients in in vivo PET assessments, autoradiography studies, PET-to-postmortem correlational analyses, and molecular simulations,[23-30] with neurons and oligodendrocytes being the major tau-positive cell type that contributed to PI-2620 PET signal.[30] In addition, we used GE180, that is, a PET tracer binding to the 18-kDa TSPO, which is overexpressed on mitochondrial membranes in activated microglia and is commonly used as a target for PET-based imaging of microglial activation. By combining resting-state fMRI-based connectivity, tau-PET and TSPO-PET in these patients, we determined (1) whether tau and microglial activation colocalize, (2) whether tau and microglial activation expand in similar spatial patterns across interconnected brain regions, and (3) whether the spatial expansion of microglial activation across connected regions parallels the distribution of tau pathology. Answering these questions will help to further clarify the pathophysiological mechanisms

underlying 4R tauopathies and their interaction, facilitating the development of therapeutic strategies that synergistically target neuroinflammation and tau pathology in these conditions.

Subjects and Methods

Participants

We included 31 subjects recruited at LMU Munich with a clinical diagnosis of possible or probable CBS ($n = 20$) or a clinical diagnosis of PSP Richardson's syndrome (PSP-RS; $n = 11$). CBS diagnosis was made according to the revised Armstrong criteria of probable CBS or the Movement Disorders Society criteria of possible PSP with predominant CBS.[31,32] PSP-RS was diagnosed following the Movement Disorder Society diagnostic criteria.[32] Inclusion criteria for this study were age older than 45 years, stable pharmacotherapy for at least 1 week before the PET examination, negative family history for Parkinson's disease and AD, and availability of three-dimensional (3D) T1-weighted structural MRI. Exclusion criteria were severe neurological or psychiatric disorders other than PSP and CBS, or positive Aβ status, as determined via expert visual read of ^{18}F-flutemetamol or ^{18}F-florbetaben amyloid-PET, or by cerebrospinal fluid analyses of Aβ levels using locally established cutoffs (ie, $A\beta_{42/40}$ ratio < 5.5% or $A\beta_{1\text{-}42}$ < 375 pg/ml), to exclude the possibility of confounding AD-type 3/4R tau pathology.

All participants underwent rs6971 single-nucleotide polymorphism assessment (see Supporting Information Methods). We previously performed a dedicated analysis to study the impact of high-, medium-, and low-affinity status on [^{18}F]GE-180 PET signal, including patients with 4R tauopathies.[33] We found that a low-affinity binding status resulted in lower [^{18}F]GE-180 signals, whereas high- and medium-affinity binders showed only minor differences in PET signals between each other. A similar result was obtained in cohorts with primary and secondary tauopathies.[22] Thus, low-affinity binders were not included in this study, and only medium- ($n = 10$) or high-affinity binders ($n = 21$) were included in the sample.

The full study protocol including all samples, MRI, 18-F-PI2620 PET, and GE180 TSPO-PET PET data analyses were approved by the local ethics committee (LMU Munich, application numbers 17-569 and 19-022) and the German radiation protection (BfS-application: Z5 22464/2017-047-K-G) authorities. The study was carried out according to the principles of the Helsinki Declaration, and written informed consent was obtained from all participants, who received no compensation for study participation. All work complied with ethical regulations for work with human participants.

Neuroimaging Acquisition

All structural MRI data were collected on 3-T SIEMENS scanners using 3D magnetization prepared rapid acquisition with gradient echo (MPRAGE) sequences. [^{18}F]PI-2620 PET and [^{18}F]GE-180 TSPO-PET were recorded in combination with computed tomography (CT) for attenuation correction on a Siemens Biograph True point 64 PET/CT or a Siemens mCT scanner (Siemens, Erlangen, Germany). PI-2620 PET was performed in a full dynamic setting (0–60 minutes post-injection), from which we extracted a 20- to 40-minute window for assessing tau load.[3] GE-180 TSPO-PET was recorded 60–80 minutes after injection to measure microglial activation. Hofmann brain phantoms were used to obtain scanner-specific filter functions, which were used to generate images with similar spatial resolution, following the Alzheimer's Disease Neuroimaging Initiative (ADNI) image harmonization procedure (https://adni.loni.usc.edu/methods/). All datasets were visually checked for artifacts and motion corrected using rigid registration.

Neuroimaging Analyses

See the Supporting Information for structural MRI and PET preprocessing. PET images were intensity normalized to mean tracer uptake of the inferior cerebellar gray matter, to determine standardized uptake value ratio (SUVR). The dentate nucleus and superior and posterior layers of the cerebellum were excluded to account for potential tau-PET positivity in cerebellar areas and in adjacent extracerebral structures. This also limits the portion of white matter included in the reference region. All brain atlas data and the inferior cerebellar reference region were further masked with binary subject-specific gray matter maps. Mean tau-PET and TSPO-PET SUVR values were extracted for each subject for the 32 subcortical and 200 cortical regions of interest (ROIs) from unsmoothed native-space PET data and z score normalized to an in-house healthy control template. Partial volume correction was not applied.

For assessing functional connectivity, we used resting-state fMRI data from 69 cognitively normal control subjects of the ADNI cohort (30 females, age on average 77.5 ± 5.9 years; all amyloid-PET negative and cognitively normal according to ADNI classifications). Ethics approval was obtained by ADNI investigators at participating ADNI sites, and all study participants provided written informed consent. These subjects were selected based on absence of objective or subjective signs of cognitive impairment and had no evidence of clinically relevant cerebral amyloid or tau pathology, as indicated by negative ^{18}F-florbetapir amyloid-PET (ie, global SUVR < 1.11) and negative ^{18}F-flortaucipir tau-PET

scans (ie, global SUVR < 1.3).[34,35] ADNI MRI scans were obtained on Siemens scanners using unified scanning protocols. T1-weighted structural MRI was recorded using an MPRAGE sequence with 1-mm isotropic voxel-space and repetition time (TR) = 2300 ms. For functional MRI, for each subject a total of 200 resting-state fMRI volumes were recorded using a 3D echoplanar imaging (EPI) sequence in 3.4-mm isotropic voxel resolution with TR/TE/flip angle = 3000/30/90°, where TE refers to Echo Time.

To determine functional connectivity, we warped the 232 cortical and subcortical ROIs for tau-PET analyses to denoised and preprocessed fMRIs in native EPI space, by combining the linear EPI to T1 and nonlinear T1 to MNI transformation parameters (see Supporting Information for fMRI preprocessing). ROI maps in EPI space were masked with subject-specific gray matter. Fisher *z*-transformed Pearson-Moment correlations between time series averaged across voxels within an ROI were determined to assess subject-specific functional connectivity matrices. Functional connectivity data were averaged across all 69 ADNI subjects to determine group-average functional connectivity matrices matching the PET analyses.

Statistics

To determine abnormality of tau-PET and TSPO-PET SUVR data, we generated ROI-wise *z* scores using an in-house sample of healthy controls for each tracer (tau-PET controls: age 70.1 ± 10.5 years, female/male = 10/8; TSPO controls: 71.1 ± 6.8 years, female/male = 8/9). *z* scores were determined as abnormal when falling above a threshold of 1.645. To determine spatial patterns of abnormal tau-PET and TSPO-PET, we mapped the probability of regional cortical and subcortical PET SUVR *z* scores falling above a threshold of 1.645 within the cohort of 31 4R tau patients.

To test the association between connectivity and interregional tau-TSPO PET covariance, we first determined the interregional functional connectivity the $n = 69$ healthy amyloid- and tau-negative control subjects from the ADNI cohort. Using the ROI-wise PET *z* scores determined in the cohort of 31 4R tauopathy patients, we then performed partial correlations in tau-PET or TSPO-PET *z* scores between any two pairs of ROIs, adjusting for age and sex.

To test tau propagation and neuroinflammation spatial expansion patterns, we determined patient-specific tau epicenters. This analysis was run at the subject level, that is, we defined each PSP-RS and CBS patient's tau epicenter as 5% of individual regions with the highest tau-PET *z* scores (even regions within the normal range values). We used a conservative threshold of 5% to include the very early regions affected by tau pathology. We assessed seed-based connectivity of each subject tau epicenter using the functional connectivity template obtained in ADNI healthy control samples (as for the previous analysis). We then tested for each subject whether seed-based tau epicenter connectivity predicted brain-wide tau-PET and TSPO-PET patterns using linear regression. Subject-level standardized regression coefficients (ie, β values) were then extracted as proxy measures of connectivity-associated distribution of tau and neuroinflammation.

Next, we tested whether the tau or neuroinflammation load in the tau epicenter determined the degree to which tau or neuroinflammation spatially progress throughout the brain. To this end, we tested whether higher tau-PET or TSPO-PET abnormality in the tau epicenter predicted stronger subject-level tau-PET or TSPO-PET signal across connected brain regions (ie, higher subject-level β values of the association between tau epicenter connectivity and tau-PET or TSPO-PET uptake in the rest of the brain) using linear regression, controlling for age, sex, and diagnosis.

Lastly, we tested whether the spatial expansion of microglial activation across connected regions follows and parallels the distribution of tau pathology. To this end, we employed a preestablished approach[3] and grouped nonepicenter brain regions into four subject-specific quartiles, depending on their connectivity level to the tau epicenter, and calculated individual average *z* scores across regions for each PET modality.

Results

Sample characteristics are shown in Table 1. In line with our previous work, across patients the highest tau-PET abnormality was found in the basal ganglia and primary sensorimotor cortex (Fig. 1A). Similarly, the strongest TSPO-PET abnormality was also detected in the basal ganglia and frontal brain regions (Fig. 1B). The group-level spatial patterns of tau-PET and TSPO-PET abnormality (ie, Fig. 1A,B) showed a moderate

TABLE 1 *Demographic and clinical information of 4R tauopathy patients*

Age, y	70.0 ± 8.2
Sex, F/M	17/14
PSP-RS/Aβ-negative CBS	11/20
MoCA score	22.9 ± 4.6
SEADL	64.1 ± 15.2
TSPO binding affinity, medium/high	10/21

Abbreviations: 4R, 4-repeat; F, female; M, male; PSP, progressive supranuclear palsy; RS, Richardson's syndrome; CBS, corticobasal syndrome; MoCA, Montreal Cognitive Assessment Scale; SEADL, Schwab and England Activities of Daily Living Scale; TSPO, translocator protein.

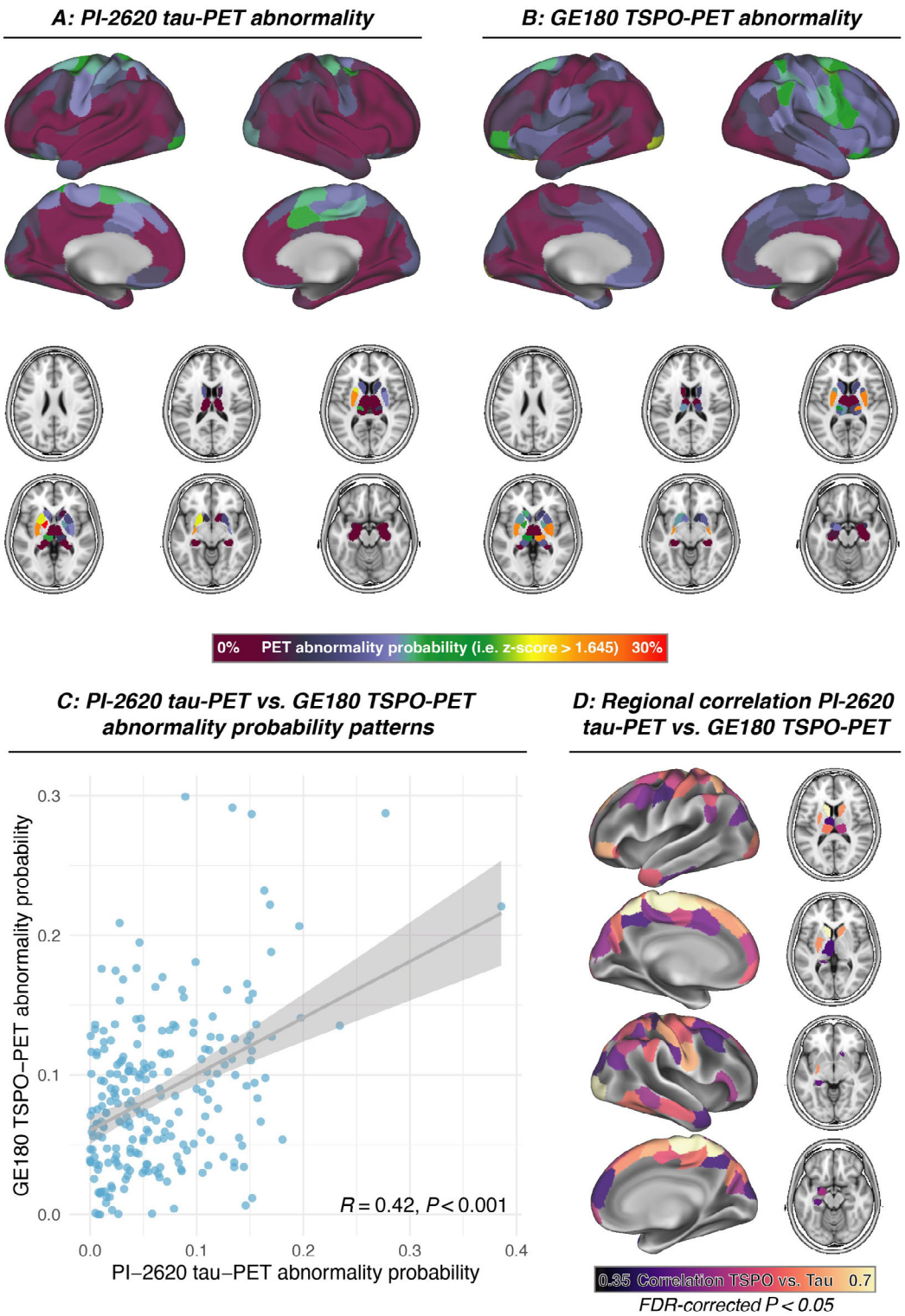

FIG. 1. Tau-PET and TSPO-PET abnormality patterns in patients versus controls. (**A**, **B**) Surface rendering of PI-2620 tau-PET and GE180 TSPO-PET abnormality defined as the probability of regional PET *z* scores (ie, standardized uptake value ratios adjusted against healthy controls) falling above a threshold of 1.645. (**C**) Spatial correlation of TSPO-PET and tau-PET abnormality patterns shown in (**A**) and (**B**). (**D**) ROI-wise correlation between TSPO-PET and tau-PET across subjects, corrected for multiple comparisons (ie, FDR, $P < 0.05$). FDR, false discovery rate; PET, positron emission tomography; ROI, region of interest; TSPO, translocator protein. [Color figure can be viewed at wileyonlinelibrary.com]

correlation ($r = 0.42$, $P < 0.001$; Fig. 1C), and regional across-subject analyses showed widespread moderate to strong correlations between TSPO and tau-PET in cortical and subcortical regions (Fig. 1D) after false discovery rate correction for multiple comparisons. Individual coefficients of ROI-wise correlations between TSPO-

PET and PI2620 PET z scores were significantly higher than zero ($P < 0.001$) and did not differ between patients with PSP and patients with CBS ($P = 0.35$; Fig. 1A), suggesting that tau deposition and neuroinflammation are spatially correlated on the subject level. In the CBS group, the laterality of the clinical syndrome (ie, left vs. right) was not associated with the correlation between tau-PET and TSPO-PET z scores ($r = 0.02$, $P = 0.94$; Supporting Information Fig. S1B).

Association Between Connectivity and Interregional Covariance in Tau-PET and TSPO-PET

First, we assessed whether tau and neuroinflammation levels as measured via PI-2620 and GE180 PET correlate among functionally connected brain regions (see Supporting Information Fig. S2). We found that more strongly connected brain regions showed higher covariance in both tau-PET ($\beta = -0.434$, $P < 0.001$, $R^2 = 0.215$; Fig. 2A) and TSPO-PET ($\beta = -0.489$, $P < 0.001$, $R^2 = 0.239$; Fig. 2B). Similarly, ROI pairs with high covariance in tau-PET also showed high covariance in TSPO-PET ($\beta = 0.414$, $P < 0.001$, $R^2 = 0.171$; Fig. 2C).

Next, we tested whether tau and neuroinflammation in highly connected hub regions are most influential for brain-wide tau and TSPO-PET patterns. We determined the global connectivity of each ROI (ie, average connectivity-based distance of a given ROI to all remaining ROIs), as well as the average tau-PET and TSPO-PET covariance between a given ROI and the rest

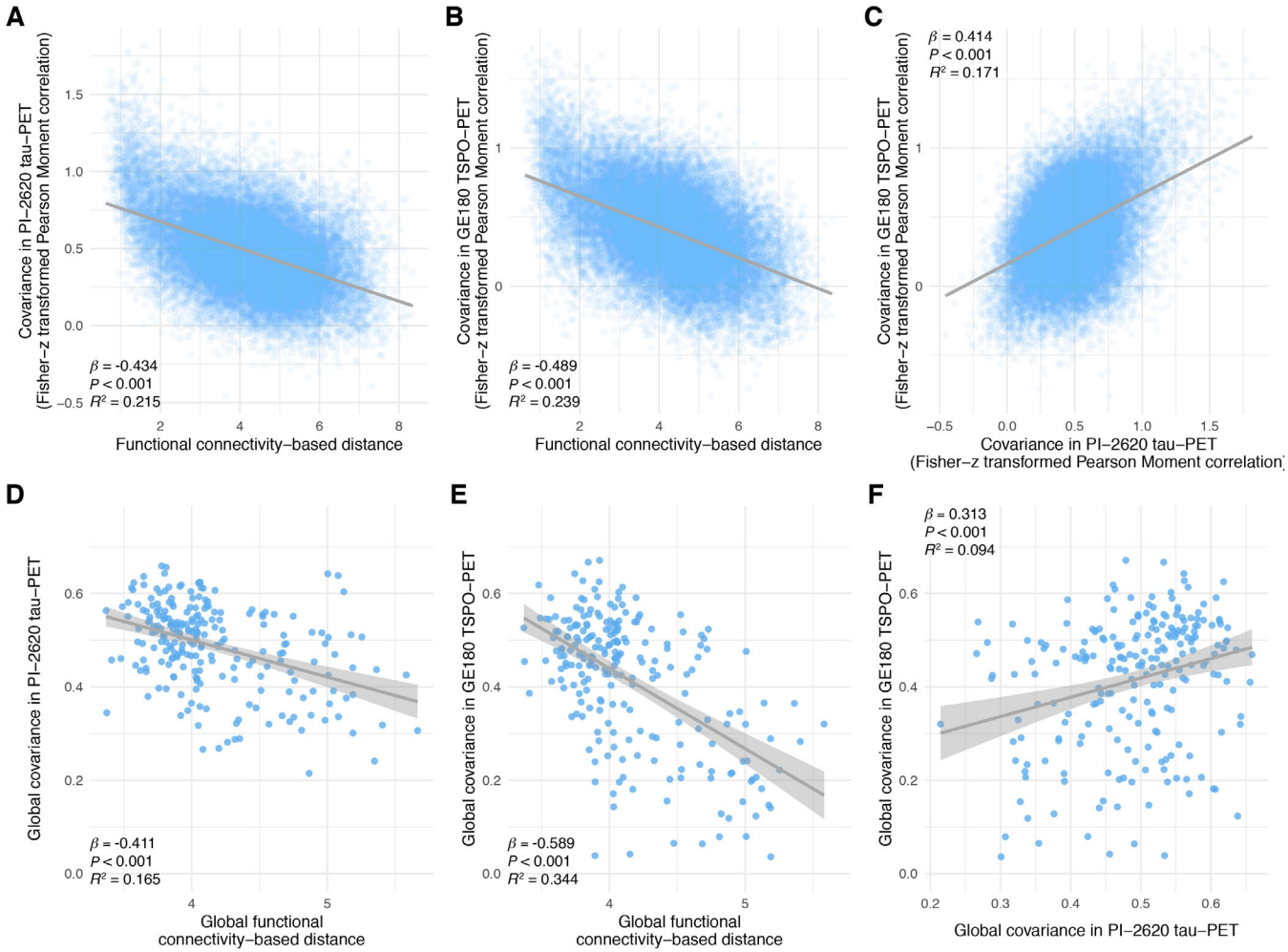

FIG. 2. Associations between TSPO-PET, tau-PET, and functional magnetic resonance imaging (fMRI) connectivity. (**A**, **B**) Scatterplots illustrating the association between functional connectivity-based distance and interregional covariance in PI-2720 tau-PET z scores (**A**) or covariance in GE180 TSPO-PET z scores (**B**), showing that functionally connected brain regions show correlated tau and neuroinflammation levels. (**C**) Association between covariance in PI-2620 tau-PET and covariance in GE180 TSPO-PET, showing that regions with correlated tau also show correlated neuroinflammation. (**D**, **E**) When assessing whether brain hubs (ie, globally connected brain regions) are influential for brain-wide tau and neuroinflammation patterns, we found that more globally connected regions (x-axis) showed higher global covariance in tau-PET (**D**) or TSPO-PET (**E**). (**F**) Scatterplot showing the association between the global interregional covariance in tau-PET and TSPO-PET. PET, positron emission tomography; TSPO, translocator protein. [Color figure can be viewed at wileyonlinelibrary.com]

of the brain. Supporting the view that globally connected hubs are influential for tau-PET and TSPO-PET distribution patterns, we found that stronger hub-ness (ie, shorter global connectivity-based distance) was linked to higher global covariance in both tau-PET ($\beta = -0.411$, $P < 0.001$, $R^2 = 0.165$; Fig. 2D) and TSPO-PET ($\beta = -0.589$, $P < 0.001$, $R^2 = 0.344$; Fig. 2E). Similarly, regions with high global covariance in tau-PET showed high global covariance in TSPO-PET ($\beta = 0.313$, $P < 0.001$, $R^2 = 0.094$; Fig. 2F). These results remained fully consistent when adjusting for TSPO binding affinity, with a strong association between covariance in TSPO-PET and connectivity ($b = -0.464$, $R^2 = 0.216$, $P < 0.001$) or covariance in tau-PET ($b = 0.373$, $R^2 = 0.139$, $P < 0.001$).

Further, to determine whether our results are confounded by spatial proximity of neighboring regions, which may also show high connectivity among each other, we reassessed the association between functional connectivity and covariance in tau-PET or TSPO-PET, controlling for interregional Euclidean distance between ROIs. We obtained fully congruent results, with significant associations between functional connectivity and covariance in tau-PET ($\beta = -0.382$, $P < 0.001$) and TSPO-PET ($\beta = -0.468$, $P < 0.001$), as well as between covariance in TSPO versus tau-PET ($\beta = 0.322$, $P < 0.001$). These results suggest that the cofluctuating levels in tau and TSPO-PET between connected regions are not merely a reflection of spatial proximity.

Finally, as explorative analysis, we tested the associations within diagnostic subgroups, we found (1) a significant association between connectivity-based distance and covariance in tau-PET for the PSP ($\beta = -0.38$, $P < 0.001$) and CBS ($\beta = -0.45$, $P < 0.001$) groups; (2) an association between connectivity-based distance and covariance in TSPO-PET for PSP ($\beta = -0.35$, $P < 0.001$) and CBS ($\beta = -0.43$, $P < 0.001$); and (3) an association between covariance in tau-PET and covariance in TSPO-PET for PSP ($\beta = 0.27$, $P < 0.001$) and CBS groups ($\beta = 0.43$, $P < 0.001$), in line with the view that regions with correlated tau-PET levels also show correlated TSPO-PET.

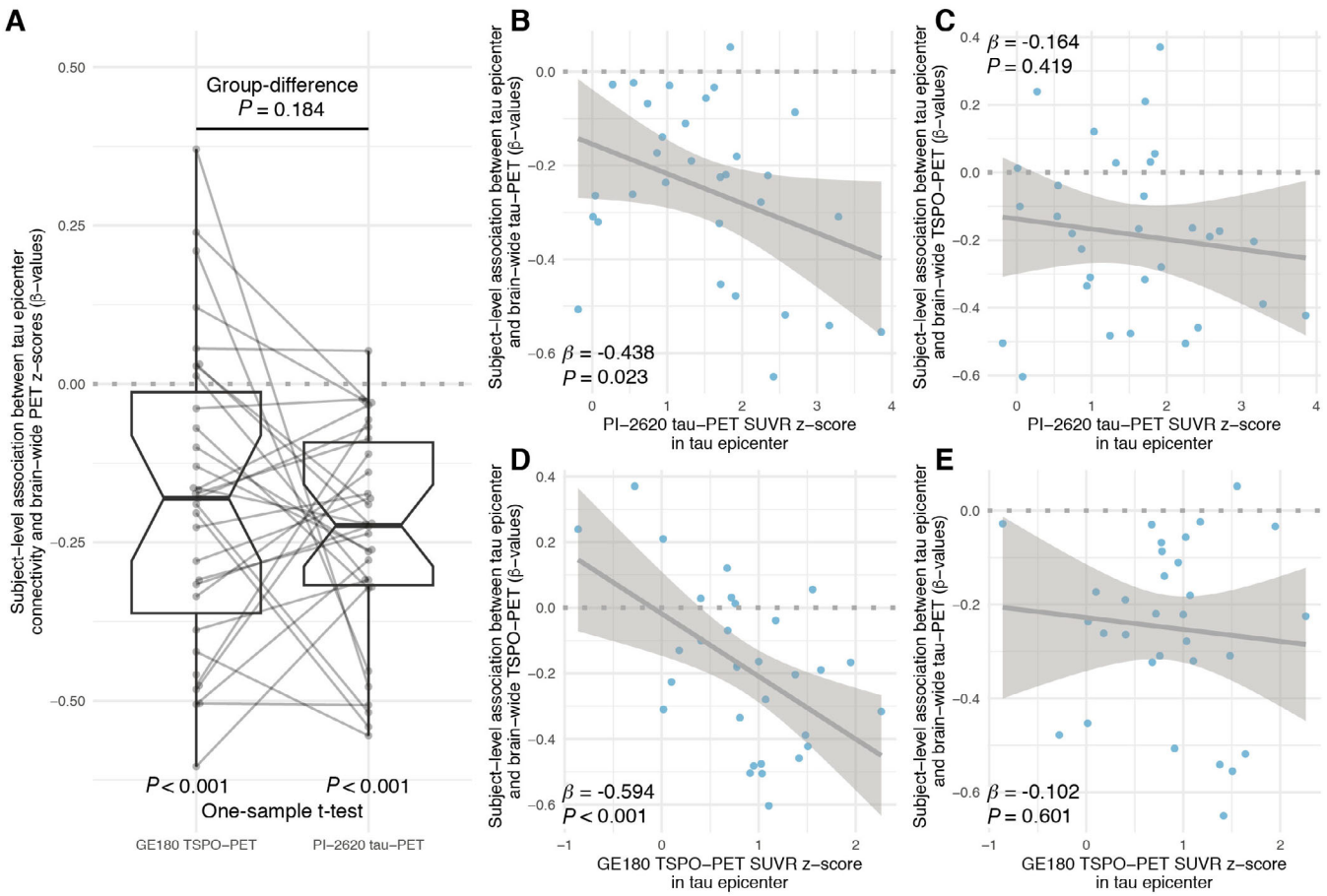

FIG. 3. Tau and neuroinflammation determine their respective progression patterns. (**A**) Regression-derived β values of the subject-level association between tau epicenter connectivity and GE180 TSPO-PET (left) and PI-2620 tau-PET in nonepicenter regions. (**B**, **C**) Higher tau-PET *z* scores in the epicenter were linked to a stronger association between epicenter connectivity and tau (**B**), but not TSPO-PET (**C**). (**D**, **E**) Higher TSPO-PET *z* scores in the epicenter were related to a stronger association between epicenter and TSPO (**D**), but not tau-PET (**E**). PET, positron emission tomography; SUVR, standardized uptake value ratio; TSPO, translocator protein. [Color figure can be viewed at wileyonlinelibrary.com]

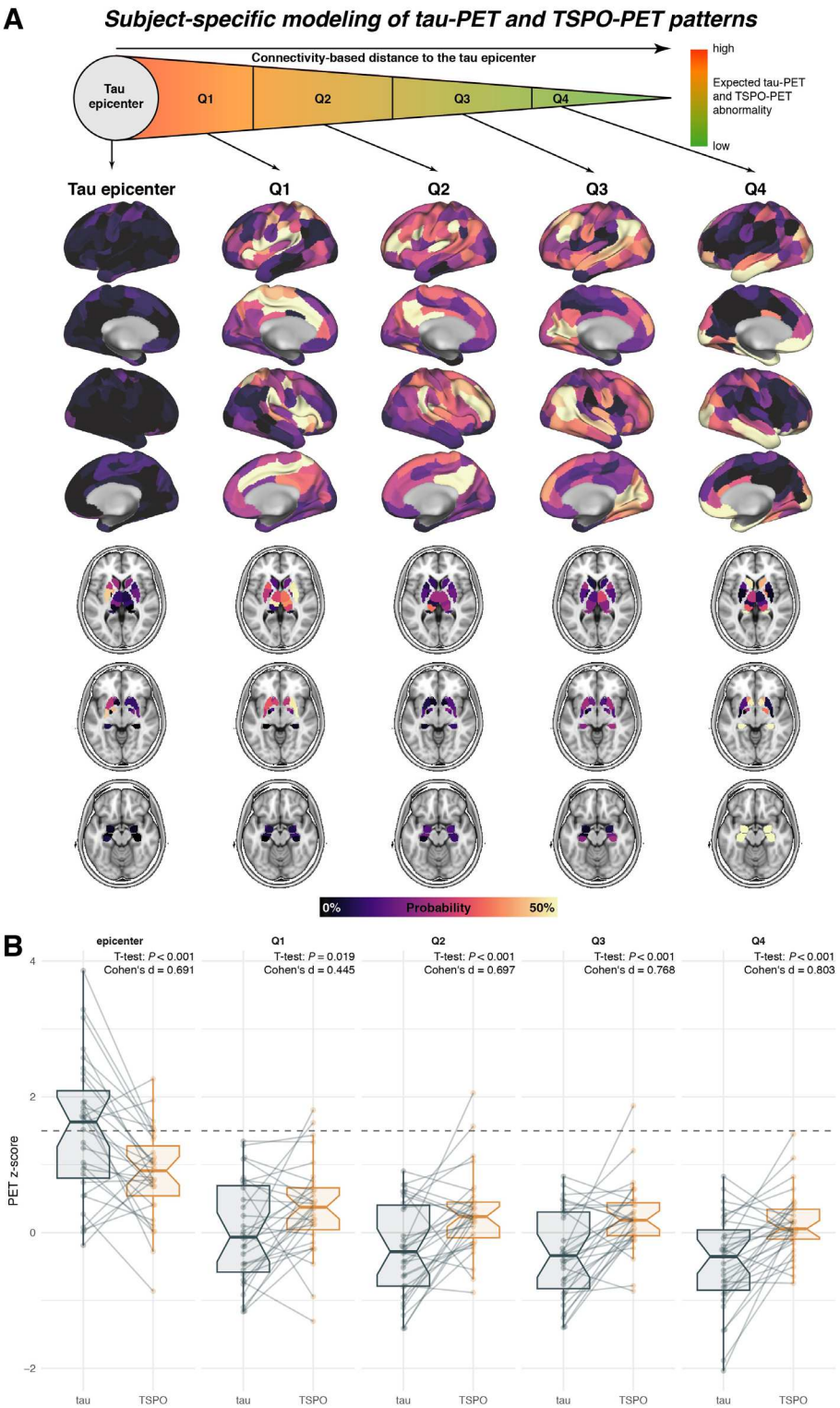

FIG. 4. Microglial activation (TSPO-PET) progression spatially parallels tau distribution detectable with PI-2620 PET. (**A**) Using subject-level tau-PET data, we determined for each patient the subcortical tau epicenter, that is, defined as 5% of ROIs with highest tau-PET standardized uptake value ratios. The remaining regions of interest (ROIs) were grouped for each subject into quartiles, depending on connectivity strength to the subject-specific tau epicenter. (**B**) For each quartile, we compared TSPO-PET and PI2620-PET values. Within the tau epicenter, tau-PET *z* scores were higher than TSPO-PET *z* scores (Cohen's $d = 0.691$, $P < 0.001$). In contrast, TSPO-PET *z* scores were higher than tau-PET *z* scores across Q1/Q2/Q3/Q4 ROIs. PET, positron emission tomography; TSPO, translocator protein. [Color figure can be viewed at wileyonlinelibrary.com]

Tau- and TSPO-PET Signal in Local Epicenters Is Highly Associated with Respective Tracer Uptake in Highly Connected Regions

Second, we tested whether the expansion of tau and neuroinflammation follows the connections of tau epicenters in which tau is assumed to emerge first. Patient-specific tau epicenters were identified as the 5% of ROIs with highest baseline tau-PET z scores and included in seed-based connectivity analyses using the functional connectivity template obtained in ADNI healthy controls (Supporting Information Fig. S2C). The linear regression models on the seed-based tau epicenter connectivity and tau-PET patterns in the rest of the brain identified that the distribution of β values was significantly lower than zero (mean/SD = −0.25/0.81, minimum/maximum [min/max] = −0.65/0.05, 95% confidence interval [CI] = −0.32/−0.18, $T = -7.53$, $P < 0.001$; Fig. 3A). This suggests that regions that are more closely connected to the epicenter (ie, shorter connectivity-based distance) show higher tau-PET uptake. Congruent results were obtained for the association between tau epicenter connectivity and TSPO-PET uptake in the rest of the brain (mean/SD = −0.18/0.24, min/max = −0.6/0.37, 95% CI = −0.27/−0.09, $T = -4.19$, $P < 0.001$; Fig. 3A), and this association was not different in high- versus medium-affinity TSPO binders ($P = 0.52$). No significant differences were obtained in β-value distributions for the prediction of tau-PET or TSPO-PET deposition patterns using tau epicenter connectivity ($T = 1.360$, $P = 0.184$; Fig. 3A).

Similarly for the previous point, to determine whether spatial proximity of neighboring regions influences this result, we reran the analyses controlling for Euclidean distance to the respective epicenter. Here, we detected fully congruent results, showing that the linear regression models on the seed-based tau epicenter connectivity and tau-PET patterns in the rest of the brain identified that the distribution of β values was significantly lower than zero (mean/SD = −0.20/0.18, min/max = −0.56/0.15, 95% CI = −0.27/−0.13, $T = -6.02$, $P < 0.001$). In line with our main results that were not controlled for Euclidean distance, this suggests that regions that are more closely connected to the epicenter (ie, shorter connectivity-based distance) show higher tau-PET uptake. Congruent results were obtained for the association between tau epicenter connectivity and TSPO-PET uptake in the rest of the brain (mean/SD = −0.14/0.23, min/max = −0.52/0.29, 95% CI = −0.23/−0.06, $T = -3$–44, $P = 0.002$). No significant differences were obtained in β-value distributions for the prediction of tau-PET or TSPO-PET deposition patterns using tau epicenter connectivity ($T = 1.060$, $P = 0.293$).

Tau and Neuroinflammation Determine Their Respective Progression Patterns

Next, we tested whether the intensity of tau or TSPO PET signal within the tau epicenter predicts the degree to which tau or neuroinflammation spatially progress throughout the brain. We found that higher tau-PET z scores in the epicenter were linked to a stronger association between epicenter connectivity and tau ($b = -0.438$, $P = 0.023$; Fig. 3B), but not TSPO-PET ($b = -0.164$, $P = 0.419$; Fig. 3C). In contrast, higher TSPO-PET in the epicenter was related to a stronger association between epicenter and TSPO ($b = -0.594$, $P < 0.001$; Fig. 3D), but not tau-PET ($b = -0.102$, $P = 0.601$; Fig. 3E). Results remained consistent when exploratorily adjusting for TSPO binding affinity.

The Spatial Progression of Neuroinflammation Parallels Tau Distribution

Lastly, we aimed to determine whether the spatial expansion of microglial activation across connected regions follows and parallels the distribution of tau pathology, that is, whether tau-PET or TSPO-PET increase more than one another across regions connected to the tau epicenter. We determined four subject-specific quartiles and grouped nonepicenter brain regions accordingly (ie, Q1 = strongest connectivity to the tau epicenter versus Q4 = weakest connectivity to the tau epicenter; Fig. 4A). Within the tau epicenter, we found that tau-PET z scores were higher than TSPO-PET z scores (Cohen's $d = 0.691$, $P < 0.001$; Fig. 4B). In contrast, TSPO-PET z scores were higher than tau-PET z scores across Q1/Q2/Q3/Q4 ROIs (Cohen's $d = 0.445/0.697/0.768/0.803$, $P = 0.019/<0.001/<0.001/<0.001$; Fig. 4B). For each modality-specific value, the epicenter showed the highest z scores followed by Q1, with decreasing values in Q2, Q3, and Q4.

Discussion

Our results suggest that microglial activation does not only colocalize with elevated tau levels in patients with 4R tauopathies but also follows similar progression patterns as tau pathology and distributes primarily across brain regions that are functionally connected to each other. Importantly, our findings indicate that microglial activation captured with TSPO-PET in regions connected to tau pathology epicenters parallels tau detectable with PI-2620 PET. Our approach ensures the generalizability of our results across 4R tauopathies, because the clinical and pathoanatomical variability (ie, PSP and CBD, laterality) within the group of interest maximizes the likelihood that the observed associations between TSPO and 18F-PI-2620 PET signals reflect not only pathoanatomical differences between a particular disease-related pattern and controls, but rather 4R tau deposition and corresponding neuroinflammation, regardless of their specific localization in the brain.

First, we tested whether tau and microglial activation colocalize. As for previous reports in primary

tauopathies,[10,22] as well as AD,[21,36] which indicated that tau is closely related to increased microglial activation, our findings confirm spatial colocalization and covariance of tau and microglial activation in patients with PSP and CBS. In addition, for the first time in patients with primary 4R tauopathies, our study shows that not only tau pathology but also neuroinflammation distributes primarily across brain regions that are functionally connected to each other, in line with the hypothesis that tau spreads across connected brain regions and that neuroinflammation may follow similar progression patterns. This adds to previous imaging studies in patients with AD, showing that microglial activation is correlated across connected brain regions.[37,38] Specifically, highly connected brain hubs showed stronger global covariance in both tau-PET and TSPO-PET, suggesting that regions with brain-wide connectivity may act as key relay stations for the expansion of tau and neuroinflammation across connected regions in 4R tauopathies. In other words, regions that have a higher global connectivity with the rest of the brain have stronger covariance of tau and inflammation, suggesting that if early tau pathology and microglial activation are localized in these highly connected regions, they are more likely to progress and spread to the rest of the brain, respectively. Regional differences in gene expression[39] and microglial responses to pathological triggers or clearance capacity of dysfunctional synapses and neurons[40,41] may also contribute to regional variability in tau pathology accumulation and inflammatory responses. Brain regions differ in microglia abundance, with subcortical regions having more resident microglia,[42] which may contribute to the increased vulnerability of specific areas and the connected ones for early tau accumulation and spread.

Second, we investigated whether tau and microglial activation expand in similar spatial patterns across interconnected brain regions. Previous imaging studies in patients with 4R tauopathies and AD[3,43] suggested that tau accumulation starts in specific epicenters that define the subsequent progression pattern of tau pathology. Here, we determined patient-specific tau epicenters (ie, regions with highest baseline tau-PET z scores) and tested whether seed-based tau epicenter connectivity predicted brain-wide tau-PET and TSPO-PET patterns. Our results showed that both tau-PET and TSPO-PET patterns overlap with the connectivity pattern of the tau epicenter, suggesting that regions that are more closely connected to the epicenter, with shorter connectivity-based distance, show higher tau and neuroinflammation levels. Specifically, tau-PET signal in tau-epicenter regions was associated with tau-PET signal in connected regions, and similarly high TSPO-PET signal in the same tau-epicenter regions was associated with high TSPO-PET signal in the rest of the connected regions. Similar to tau accumulation and spreading patterns, we showed that inflammation progression can be predicted at the individual level based on the inflammation levels in tau epicenters and their normative connectivity patterns. Thus, the cross-sectionally estimated sequence in which inflammation progresses across the brain parallels that of tau distribution, that is, largely following the functional connectivity pattern of the sites in which tau potentially emerges, supporting the view that inflammation and tau progression are closely interrelated.

Finally, we tested whether the spatial expansion of microglial activation across connected regions follows or parallels the distribution of tau pathology. Specifically, we quantified tau and TSPO-PET signals in nonepicenter brain regions divided into four subject-specific quartiles, depending on their connectivity distance from the tau epicenter given our results. A similar approach was applied in our previous work to define tau progression[3]: regions strongly connected to the tau epicenter represent regions of early spreading, whereas regions with weaker connectivity would be involved later in the disease by pathology spreading. On average, for each tracer, PET signal was higher in the epicenter and closely related regions than in those regions less connected with the epicenter (Q1 > Q2 > Q3 > Q4). This may suggest that increases in microglial activation, as assessed with TSPO-PET, in regions connected to the tau epicenter parallels tau levels detectable with tau-PET in 4R tauopathies. Although a cross-sectional PET study cannot resolve the complex biological interaction between the inflammation cascade and tau pathology in primary tauopathies, we suggest that our finding may have several alternative interpretations, including that (1) microglial activation may precede tau pathology accumulation and contribute to its spreading; or (2) early changes in tau may not be detectable with tau-PET but instigate a high immune response, including activation of microglia. Preclinical evidence in tauopathies suggests that both interpretations may be right in a bidirectional relationship between inflammation and tau pathology. In fact, inflammatory factors can initiate neuronal tau aggregation and contribute to tau spreading and tau-induced synapse dysfunction[18,40,44]; in contrast, initial tau aggregation can lead to overactivation of microglia and proinflammatory cytokine release.[40] The close relationship between microglial activation and tau pathology has been supported by studies in mouse models of neuronal tauopathies that showed how removing senescent microglia or using anti-inflammatory drugs reduces tau pathology and improves cognitive performance.[45-47] The early involvement of inflammatory pathways in the etiology of tauopathies has been suggested by genome-wide association study. For example, Jabbari et al[16] reported an association between a common variation at the LRRK2 locus and survival from symptom onset to death in patients with PSP. This relationship may be mediated by the effect of increased LRRK2 expression in microglia

proinflammatory responses,[17] promoting spread and accumulation of misfolded tau protein, analogous to AD.[40] This hypothesis is supported by the association of dysregulated expression of the microglial-related gene *CXCR4*, regional accumulation of neurofibrillary tangles, and increased risk of PSP and CBD.[48,49] The contribution of tau inclusions to microglial activation has also been supported by in vitro studies showing that the presence of tau monomers, oligomers, and fibrils leads to changes in microglial morphology and activation.[50] Interventional studies and longitudinal imaging in the presymptomatic phase of the disease course are ultimately needed to clarify whether inflammation precedes tau pathology or vice versa.

There are several limitations to our study. First, we recruited participants according to clinical diagnostic criteria, but pathology confirmation for patients included in this study was not available. We excluded patients with a positive amyloid biomarker (ie, PET or CSF) to reduce the probability to include patients with PSP and CBS clinical syndromes caused by AD, but we cannot exclude or account for other copathologies with the available biomarkers. Second, longitudinal tau-PET was available in none of the patients, although a second TSPO-PET scan was available for seven patients only, which did not allow sufficiently powered statistical analyses. Our results on tau propagation and inflammation expansion patterns should be validated in larger cohorts with multiple time points for both tracers. This would also clarify the temporal sequence of events. Similarly, our cohort's size did not enable highly powered group-specific subanalyses, although the explorative analyses within the diagnostic subgroups suggested similar results across PSP and CBD cohorts. Third, to calculate individual modality-specific z scores, we compared each patient with controls recruited locally. We included separate groups of healthy adults who underwent either TSPO-PET or tau-PET, but not both, as for limiting radiation exposure. However, the control groups were age and sex matched. Notably, comparing the two tracers, TSPO-PET signal was higher than tau-PET in all regions except for the tau epicenter. However, this may be related to different sensitivity of the tracers. Notably, tau PET tracers are characterized by "off-target" binding to monoamine oxidases expressed on reactive astrocytes and activated microglia. This could contribute to the associations observed between tau and TSPO PET tracers. However, the novel tau-PET tracer 18F-PI-2620 has been described as less affected by off-target binding to monoamine oxidases[51] than previous tau PET tracers. We did not perform partial-volume corrections on PET data from the two different tracers. Although partial-volume correction can significantly enhance the quality and reliability of PET imaging data, applying a uniform correction method across different tracers in correlation analyses could introduce tracer-specific biases and artifacts that are not present in the uncorrected data. Finally, we used TSPO-PET as a marker of microglial activation, which does not enable the differentiation between cells and microglia subtypes. Specifically, [^{18}F]GE-180 has been described with a relatively low signal-to-noise ratio and low brain penetration, as compared with other TSPO tracers. Although this may reduce its sensitivity to activated microglia, it also reduces effect sizes and increases type II errors, rather than leading to false-positive findings. In addition, the neuroinflammatory cascade in 4R tauopathies is a complex process not confined to activated microglia. Future studies with alternative and TSPO nonspecific PET tracers would elucidate further inflammation progression in these conditions.

In conclusion, our findings in primary tauopathies indicate that microglial activation spatial expansion parallels tau distribution across brain regions that are functionally connected to each other. Together with previous evidence, this suggests that tau spreading and microglial activation are closely related pathophysiological processes that may be underpinned by a synergistic and/or a causal relationship. A better understanding of the interaction between the pathological substrates in 4R tauopathies may crucially contribute to improving patient stratification in clinical trials. The combination of tau and inflammation in vivo markers could support the development of immunomodulatory strategies for disease-modifying treatments in these conditions, alone or in conjunction with treatments targeting tau pathways. ■

Acknowledgments: We thank our participant volunteers for their participation in this study and the support team who made this research study possible.

Data Availability Statement

Anonymized data may be shared upon request to the corresponding or senior author from a qualified investigator for noncommercial use, subject to restrictions according to participant consent and data protection legislation.

References

1. Coughlin DG, Dickson DW, Josephs KA, Litvan I. Progressive Supranuclear Palsy and Corticobasal Degeneration. Adv Exp Med Biol 2021;1281:151–176. https://doi.org/10.1007/978-3-030-51140-1_11
2. Stamelou M, Respondek G, Giagkou N, Whitwell JL, Kovacs GG, Höglinger GU. Evolving concepts in progressive supranuclear palsy and other 4-repeat tauopathies. Nat Rev Neurol 2021;17(10):601–620.
3. Franzmeier N, Brendel M, Beyer L, Slemann L, Kovacs GG, Arzberger T, et al. Tau deposition patterns are associated with functional connectivity in primary tauopathies. Nat Commun 2022;13(1):1–18.

4. Kovacs GG, Lukic MJ, Irwin DJ, Arzberger T, Respondek G, Lee EB, et al. Distribution patterns of tau pathology in progressive supranuclear palsy. Acta Neuropathol 2020;140(2):99–119.
5. Dutt S, Binney RJ, Heuer HW, Luong P, Attygalle S, Bhatt P, et al. Progression of brain atrophy in PSP and CBS over 6 months and 1 year. Neurology 2016;87(19):2016–2025.
6. Robinson JL, Yan N, Caswell C, Xie SX, Suh E, Van Deerlin VM, et al. Primary tau pathology, not Copathology, correlates with clinical symptoms in PSP and CBD. J Neuropathol Exp Neurol 2020; 79(3):296–304.
7. Höglinger GU, Schöpe J, Stamelou M, Kassubek J, del Ser T, Boxer AL, et al. Longitudinal magnetic resonance imaging in progressive supranuclear palsy: a new combined score for clinical trials. Mov Disord 2017;32(6):842–852.
8. Malpetti M, Passamonti L, Jones PS, Street D, Rittman T, Fryer TD, et al. Neuroinflammation predicts disease progression in progressive supranuclear palsy. J Neurol Neurosurg Psychiatry 2021;92(7): 769–775.
9. Palleis C, Sauerbeck J, Beyer L, Harris S, Schmitt J, Morenas-Rodriguez E, et al. In vivo assessment of Neuroinflammation in 4-repeat Tauopathies. Mov Disord 2021;36(4):883–894.
10. Malpetti M, Passamonti L, Rittman T, Jones PS, Vázquez Rodríguez P, Bevan-Jones WR, et al. Neuroinflammation and tau Colocalize in vivo in progressive Supranuclear palsy. Ann Neurol 2020;88(6):1194–1204.
11. Alster P, Madetko N, Koziorowski D, Friedman A. Microglial activation and inflammation as a factor in the pathogenesis of progressive Supranuclear palsy (PSP). Front Neurosci 2020;2:14.
12. Gerhard A, Trender-Gerhard I, Turkheimer F, Quinn NP, Bhatia KP, Brooks DJ. In vivo imaging of microglial activation with [11C]-PK11195 PET progresive supranuclear palsy. Mov Disord 2006;21(1):89–93.
13. Gerhard A, Watts J, Trender-Gerhard I, Turkheimer F, Banati RB, Bhatia K, et al. In vivo imaging of microglial activation with [11C] (R -PK11195) PET in corticobasal degeneration. Mov Disord 2004; 19(10):1221–1226.
14. Fernández-Botrán R, Ahmed Z, Crespo FA, Gatenbee C, Gonzalez J, Dickson DW, et al. Cytokine expression and microglial activation in progressive supranuclear palsy. Park Relat Disord 2011;17(9):683–688.
15. Ishizawa K, Dickson DW. Microglial activation parallels system degeneration in progressive supranuclear palsy and corticobasal degeneration. J Neuropathol Exp Neurol 2001;60(6):647–657.
16. Jabbari E, Koga S, Valentino RR, Reynolds RH, Ferrari R, Tan MMX, et al. Genetic determinants of survival in progressive supranuclear palsy: a genome-wide association study. Lancet Neurol 2020;20:107–116.
17. Moehle MS, Webber PJ, Tse T, Sukar N, Standaert DG, Desilva TM, et al. LRRK2 inhibition attenuates microglial inflammatory responses. J Neurosci 2012;32(5):1602–1611.
18. Maphis N, Xu G, Kokiko-Cochran ON, Jiang S, Cardona A, Ransohoff RM, et al. Reactive microglia drive tau pathology and contribute to the spreading of pathological tau in the brain. Brain 2015;138(6):1738–1755.
19. Wang C, Fan L, Khawaja RR, Liu B, Zhan L, Kodama L, et al. Microglial NF-κB drives tau spreading and toxicity in a mouse model of tauopathy. Nat Commun 2022;13(1):1969.
20. Biel D, Suárez-Calvet M, Hager P, Rubinski A, Dewenter A, Steward A, et al. sTREM2 is associated with amyloid-related p-tau increases and glucose hypermetabolism in Alzheimer's disease. EMBO Mol Med [Internet] 2023;15(2):e16987.
21. Pascoal TA, Benedet AL, Ashton NJ, Kang MS, Therriault J, Chamoun M, et al. Microglial activation and tau propagate jointly across Braak stages. Nat Med 2021;27(9):1592–1599.
22. Finze A, Biechele G, Rauchmann BS, Franzmeier N, Palleis C, Katzdobler S, et al. Individual regional associations between Aβ-, tau- and neurodegeneration (ATN) with microglial activation in patients with primary and secondary tauopathies. Mol Psychiatry 2023;28:4438–4450.
23. Brendel M, Barthel H, van Eimeren T, Marek K, Beyer L, Song M, et al. Assessment of 18 F-PI-2620 as a biomarker in progressive Supranuclear palsy. JAMA Neurol 2020;77(11):1408.
24. Franzmeier N, Brendel M, Beyer L, Arzberger T, Kovacs GG, Rubinski A, et al. Tau spreads across connected brain regions in progressive supranuclear palsy and corticobasal syndrome. Alzheimers Dement 2021;17(S4):1–6.
25. Künze G, Kümpfel R, Rullmann M, Barthel H, Brendel M, Patt M, et al. Molecular simulations reveal distinct energetic and kinetic binding properties of [18 F]PI-2620 on tau filaments from 3R/4R and 4R Tauopathies. ACS Chem Neurosci 2022;13(14):2222–2234.
26. Malarte ML, Gillberg PG, Kumar A, Bogdanovic N, Lemoine L, Nordberg A. Discriminative binding of tau PET tracers PI2620, MK6240 and RO948 in Alzheimer's disease, corticobasal degeneration and progressive supranuclear palsy brains. Mol Psychiatry 2023;28(3):1272–1283.
27. Song M, Scheifele M, Barthel H, van Eimeren T, Beyer L, Marek K, et al. Feasibility of short imaging protocols for [18F]PI-2620 tau-PET in progressive supranuclear palsy. Eur J Nucl Med Mol Imaging 2021;48(12):3872–3885.
28. Song M, Beyer L, Kaiser L, Barthel H, van Eimeren T, Marek K, et al. Binding characteristics of [18F]PI-2620 distinguish the clinically predicted tau isoform in different tauopathies by PET. J Cereb Blood Flow Metab 2021;41(11):2957–2972.
29. Palleis C, Brendel M, Finze A, Weidinger E, Bötzel K, Danek A, et al. Cortical [18 F]PI-2620 binding differentiates Corticobasal syndrome subtypes. Mov Disord 2021;36(9):2104–2115.
30. Slemann L, Gnörich J, Hummel S, Bartos LM, Klaus C, Kling A, et al. Neuronal and oligodendroglial but not astroglial tau translates to in vivo tau-PET signals in primary tauopathies. bioRxiv 2024. https://doi.org/10.1101/2024.05.04.592508
31. Armstrong MJ, Litvan I, Lang AE, Bak TH, Bhatia KP, Borroni B, et al. Criteria for the diagnosis of corticobasal degeneration. Neurology 2013;80(5):496–503.
32. Höglinger GU, Respondek G, Stamelou M, Kurz C, Josephs K a, Lang AE, et al. Clinical diagnosis of progressive supranuclear palsy: the movement disorder society criteria. Mov Disord 2017;32(6): 853–864.
33. Vettermann FJ, Harris S, Schmitt J, Unterrainer M, Lindner S, Rauchmann B-S, et al. Impact of TSPO receptor polymorphism on [18F]GE-180 binding in healthy brain and pseudo-reference regions of Neurooncological and neurodegenerative disorders. Life (Basel, Switzerland) 2021;11(6):484. https://doi.org/10.3390/life11060484
34. Landau SM, Mintun MA, Joshi AD, Koeppe RA, Petersen RC, Aisen PS, et al. Amyloid deposition, hypometabolism, and longitudinal cognitive decline. Ann Neurol 2012;72(4):578–586.
35. Maass A, Landau S, Horng A, Lockhart SN, Rabinovici GD, Jagust WJ, et al. Comparison of multiple tau-PET measures as biomarkers in aging and Alzheimer's disease. Neuroimage 2017;157: 448–463. https://doi.org/10.1016/j.neuroimage.2017.05.058
36. Dani M, Wood M, Mizoguchi R, Fan Z, Walker Z, Morgan R, et al. Microglial activation correlates in vivo with both tau and amyloid in Alzheimer's disease. Brain 2018;141:2740–2754.
37. Rauchmann B, Brendel M, Franzmeier N, Trappmann L, Zaganjori M, Ersoezlue E, et al. Microglial activation and connectivity in Alzheimer disease and aging. Ann Neurol [Internet] 2022; 92(5):768–781.
38. Passamonti L, Tsvetanov KA, Jones PS, Bevan-Jones WR, Arnold R, Borchert RJ, et al. Neuroinflammation and functional connectivity in Alzheimer's disease: interactive influences on cognitive performance. J Neurosci 2019;39(36):7218–7226.
39. Tan Y-L, Yuan Y, Tian L. Microglial regional heterogeneity and its role in the brain. Mol Psychiatry 2020;25(2):351–367.
40. Vogels T, Murgoci AN, Hromádka T. Intersection of pathological tau and microglia at the synapse. Acta Neuropathol Commun 2019; 7(1):109.
41. De Biase LM, Bonci A. Region-specific phenotypes of microglia: the role of local regulatory cues. Neuroscientist 2019;25(4):314–333.
42. Ochocka N, Kaminska B. Microglia diversity in healthy and diseased brain: insights from single-cell omics. Int J Mol Sci 2021; 22(6):3027.

43. Franzmeier N, Dewenter A, Frontzkowski L, Dichgans M, Rubinski A, Neitzel J, et al. Patient-centered connectivity-based prediction of tau pathology spread in Alzheimer's disease. Sci Adv 2020;6(48):eabd1327.

44. Perea JR, Llorens-Martín M, Ávila J, Bolós M. The role of microglia in the spread of tau: relevance for Tauopathies. Front Cell Neurosci 2018;12:1–8.

45. Yoshiyama Y, Higuchi M, Zhang B, Huang SM, Iwata N, Saido TCC, et al. Synapse loss and microglial activation precede tangles in a P301S Tauopathy mouse model. Neuron 2007;53(3):337–351.

46. Asai H, Ikezu S, Tsunoda S, Medalla M, Luebke J, Haydar T, et al. Depletion of microglia and inhibition of exosome synthesis halt tau propagation. Nat Neurosci 2015;18(11):1584–1593.

47. Bussian TJ, Aziz A, Meyer CF, Swenson BL, van Deursen JM, Baker DJ. Clearance of senescent glial cells prevents tau-dependent pathology and cognitive decline. Nature 2018;562(7728):578–582.

48. Bonham LW, Karch CM, Fan CC, Tan C, Geier EG, Wang Y, et al. CXCR4 involvement in neurodegenerative diseases. Transl Psychiatry 2018;8(1):73.

49. Yokoyama JS, Karch CM, Fan CC, Bonham LW, Kouri N, Ross OA, et al. Shared genetic risk between corticobasal degeneration, progressive supranuclear palsy, and frontotemporal dementia. Acta Neuropathol 2017;133(5):825–837.

50. Morales I, Jiménez JM, Mancilla M, Maccioni RB. Tau oligomers and fibrils induce activation of microglial cells. J Alzheimers Dis 2013;37(4):849–856.

51. Kroth H, Oden F, Molette J, Schieferstein H, Capotosti F, Mueller A, et al. Discovery and preclinical characterization of [18F] PI-2620, a next-generation tau PET tracer for the assessment of tau pathology in Alzheimer's disease and other tauopathies. Eur J Nucl Med Mol Imaging [Internet] 2019;46(10):2178–2189.

Supporting Data

Additional Supporting Information may be found in the online version of this article at the publisher's web-site.

SGML and CITI Use Only
DO NOT PRINT

Author Roles

Design: M.M., S.N.R., S.H., J.L., G.U.H., M.B., and N.F.
Execution: M.M., S.N.R., S.H., M.G., J.G., A. Dewenter, A. Steward, D.B., A. Dehsarvi, F.W., N.K., E.W., C.P., S.K., R.R., R.P., B.-S.R., J.L., G.U.H., M.B., and N.F.
Analysis: M.M., S.N.R., S.H., M.B., and N.F.
Writing: M.M., S.N.R., G.U.H., M.B., and N.F.
Editing of final version of the manuscript: M.M., S.N.R., S.H., M.G., J.G., A. Stephens, A. Dewenter, A. Steward, D.B., A. Dehsarvi, F.W., A.M., N.K., E.W., C.P., S.K., R.R., R.P., B.-S.R., J.L., G.U.H., M.B., and N.F.

Financial Disclosures

The authors do not have any competing interests pertaining to this manuscript. R.P. has received honoraria for advisory boards and speaker engagements from Roche, EISAI, Eli Lilly, Biogen, Janssen-Cilag, Astra Zeneca, Schwabe, Grifols, Novo Nordisk, and Tabuk. C.P. is an inventor for a patent "Oral Phenylbutyrate for Treatment of Human 4-Repeat Tauopathies" (EP 23156122.6) filed by LMU Munich. N.F. has received honoraria for advisory boards and speaker engagements from Life Molecular Imaging, MSD, and ESAI and receives research funding from Eli Lilly. M.M. has acted as a consultant for Astex Pharmaceuticals.